ELSEVIER

Journal of Power Sources 54 (1995) 68–71

JOURNAL OF POWER SOURCES

Characterization of silver vanadium oxide cathode material by high-resolution electron microscopy

A.M. Crespi [a], P.M. Skarstad [a], H.W. Zandbergen [b]

[a] *Medtronic, Inc., 6700 Shingle Creek Parkway, Minneapolis, MN, USA*

[b] *National Centre for HREM, Laboratory of Materials Science, Delft University of Technology, Rotterdamseweg 137, 2628 AL Delft, Netherlands*

Abstract

The nature of the discharge reaction of lithium/silver vanadium oxide batteries was investigated. The lithiation of silver vanadium oxide, which has the formula $Ag_{2-y}V_4O_{11}$, proceeds by a multistep reaction, as indicated by the open-circuit voltage curve. The first step in the discharge reaction involves reduction of silver and separation of the oxide into two phases of differing composition. Electron diffraction of lithiated materials of various compositions suggests that the layered structure of the oxide is maintained, but with an increased amount of stacking disorder. High-resolution electron micrographs of lithiated $Ag_{2-y}V_4O_{11}$ at atomic resolution could not be obtained because of sample decomposition in the electron beam.

Keywords: Cathode materials; Silver; Vanadium

1. Introduction

Lithium/silver vanadium oxide batteries are the state-of-the-art power source for implantable cardiac defibrillators [1–4]. The shape of the discharge curve and high-rate capability of this system make it ideal for this application. The stepped discharged curve allows for estimation of the state of charge of the battery by simply reading the battery voltage, a feature that is desirable in an implanted medical device. One step toward understanding this battery system is to characterize the starting materials and the products of the discharge reaction. This paper is part of continuing study of the structure of silver vanadium oxide, its reactions of lithiation, and the thermodynamics of the lithium/silver vanadium oxide system [5,6].

Silver vanadium oxide cathode material has been synthesized by both a decomposition reaction between $AgNO_3$ and V_2O_5 [1], and a combination reaction between Ag_2O and V_2O_5 [5,6]. Both of these materials have the approximate formula $Ag_2V_4O_{11}$. The combination reaction, which is performed at a higher temperature, yields a more crystalline material with a needle-like crystal morphology, which is suitable for characterization by X-ray diffraction, electron diffraction, and high-resolution electron microscopy (HREM) [5,6]. The material synthesized by the decomposition method also takes on a needle-like morphology after sintering at 450 °C in air [7].

High-resolution electron microscopy has been particularly useful is discerning the details of the structure of $Ag_2V_4O_{11}$. We have reported an HREM study of $Ag_2V_4O_{11}$. Low-resolution HREM images showed the presence of silver particles on the surface of the crystals. The size and number of the particles did not grow with increasing time in the electron beam, which confirms that the silver particles were not produced by the electron beam but were already present in the sample [5]. The silver vanadium oxide did, however, become somewhat amorphous. Precipitates of silver also appeared in the $Ag_2V_4O_{11}$ crystal. The material was synthesized using a 1:2 molar ratio of Ag_2O and V_2O_5, so the presence of metallic silver in the sample implies that it is deficient in silver. The formula can therefore be written $Ag_{2-y}V_4O_{11}$. Refinement of the X-ray data, however, shows that the occupancy of Ag is 0.96(1), so the value of y must be quite small [5].

The unit cell of $Ag_{2-y}V_4O_{11}$ was determined by electron diffraction. The presence of twinning and stacking faults was also apparent from the electron diffraction pattern. The unit cell was refined using X-ray diffraction data and determined to be $a = 15.41(1)$ Å, $b = 3.5766(3)$ Å, $c = 9.564(8)$ Å, $b = 128.74(1)$ Å. HREM images along the b-axis reveal a layered structure

SSDI 0378-7753(94)02042-2

(see Fig. 1). The dark spots in the HREM image denotes heavy elements, in this case vanadium or silver. These elements cannot be distinguished from each other in this image. Two types of layers are present: single rows of blacks spots, or rows consisting of clusters of four back dots. By analogy to $Cu_xV_4O_{11}$, the single spots are probably silver and the clusters of four spots are vanadium [8]. This structure can be derived from β-$M_xV_2O_5$ by removing the VO_2 units from the sides of the tunnels [9]. The structure was refined by the Rietveld method using the X-ray diffraction data. The refinement converged on the same structure indicated by the HREM images.

Stacking faults and twinning are also apparent in the HREM images (Fig. 1). The bulk of the material has a stacking pattern designed Type I. The Type I structure had not been previously reported. The minority stacking pattern, designated Type II, resembles that of $Cu_xV_4O_{11}$ [8]. The presence of this stacking was not detectable by X-ray diffraction. Attempts to refine the X-ray data including a proportion of this structure resulted in no improvement in the structure factor.

2. Experimental

The experimental procedures used in this synthesis of $Ag_{2-y}V_4O_{11}$, HREM, and X-ray powder diffraction are described in Ref. [5]. The open-circuit voltage (OCV) measurements were performed in hermetically sealed batteries, which are described in Ref. [6]. The temperature coefficient of the OCV was determined in a Thermotron temperature chamber. The batteries were allowed to equilibrate for 2.5 h each at 70, 60, 37, 22 and −5 °C.

The lithiated samples of $Ag_{2-y}V_4O_{11}$ cathode were taken from the same batteries used for the OCV measurements. The batteries were opened in a helium-filled glove box. The cathodes were removed, washed sequentially with dried, degassed propylene carbonate and 1,2-dimethoxyethane, and dried under vacuum. Specimens for electron microscopy were obtained by crushing and mounting the crystal fragments on a copper grid covered with a carbon-coated holey film. Electron microscopy was performed with a Philips CM30T electron microscope operating at 300 kV and equipped with a 60°/35° tilt specimen holder.

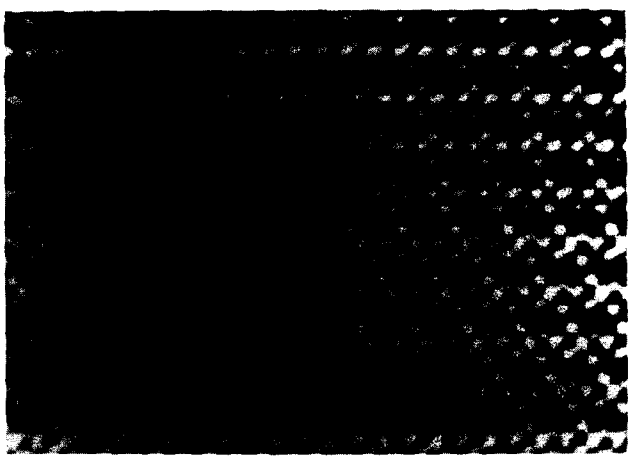

Fig. 1. High-resolution electron micrographs of $Ag_{2-y}V_4O_{11}$ in the direction of the *b*-axis, from Ref. [5].

3. Results and discussion

3.1. Thermodynamic of lithiation

The OCV and temperature coefficient of Li/Li_x-$Ag_{2-y}V_4O_{11}$ versus x appear in Fig. 2. The OCV is constant at 3.24 V in the range $0<x<2$, and at 2.6 V in the range $3<x<5.2$, which implies a heterogeneous reaction in these ranges of composition. For most binary oxide cathode materials, the constant OCV would indicate a region in which two oxide phases coexist. With the $Li/Li_xAg_{2-y}O_{11}$ system silver mobility is also a possibility, which would make it a three-component system. Thus, in regions of constant OCV three phases may coexist, metallic silver and two oxide phases. The two oxide phases may be structurally similar but differ in composition and be immiscible. X-ray diffraction of cathode discharged to 3.0 V shows the presence of metallic silver [10]. Regions of sloping OCV occur at $2<x<3$ and $5.2<x<7$. The insertion of lithium into a host structure in a single-phase reaction presumably occurs in these regions.

The temperature coefficient of the OCV also appears in Fig. 2. Note that the temperature coefficient is not constant in the regions of constant OCV, but becomes more negative with increasing x. The entropy of the discharge reaction can in some cases be calculated from $\Delta S = nF(\delta E/\delta T)_p$, where ΔS is the entropy of reaction, n the number of electrons transferred in the reaction, F the Faraday constant, E the open-circuit voltage, T the temperature, and p the pressure. In the case of

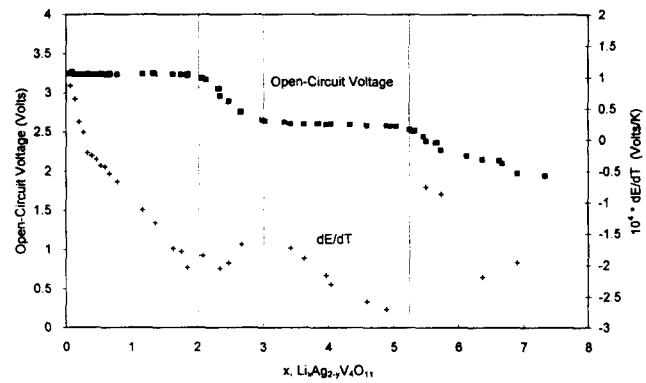

Fig. 2. Open-circuit voltage at 37 °C and the temperature coefficient of the open-circuit voltage for $Li/Li_xAg_{2-y}V_4O_{11}$ as a function of x.

heterogeneous reaction, however, the entropy as well as the OCV is expected to be constant. The changing temperature coefficient can be rationalized in terms of the temperature dependence of the width of the region in which more than one oxide phase coexists. The samples were initially allowed to equilibrate at 37 °C for one year or more. During the measurements of the temperature coefficient, the samples equilibrated for only 2.5 h at each temperature, so the cathode remained at constant composition, or in other words did not reach the equilibrium composition at that temperature. The potential that is measured is therefore not a true open-circuit potential but is a function of the charge-transfer resistance for the phases. Entropy values can reasonably be calculated in the regions of sloping OCV. A value of approximately -17 J/(K mol) is obtained for $2<x<3$, and a range of -8 to -19 J/(K mol) is obtained for $5.2<x<7$.

3.2. Discharge behaviour of $Li/Li_xAg_{2-y}V_4O_{11}$

A typical discharge curve of a $Li/Ag_{2-y}V_4O_{11}$ battery appears in Fig. 3. The battery was discharged at a low background rate with high current pulses ($\sim$25 mA/cm^{-2}) applied periodically. A measure of battery resistance, R_{dc}, was calculated from the drop in voltage that occurred during pulsing using Ohm's law. The plot of R_{dc} versus x shows a characteristic minimum at $x \approx 2.8$, with an increase for higher values of x. This minimum suggests that metallic silver may be produced at low values of x.

3.3. Structural studies of lithiated $Li_xAg_{2-y}V_4O_{11}$

The lithiated samples of $Ag_{2-y}V_4O_{11}$ ($x=2$, 3 and 5.2) consist of needle-shaped particles with a morphology similar to that of $Ag_{2-y}V_4O_{11}$. Many particles of silver ranging in size from 50 to 200 nm were observed on the outside of the particles (see Fig. 4). The amount of silver greatly exceeded the amount present in the unlithiated sample of $Ag_{2-y}V_4O_{11}$, reported in Ref. [5]. The observation of metallic silver on the outside of the particles is consistent with the results reported in Ref. [10]. The reduction of silver was also reported in Ref. [11]. In Ref. [10], silver was detected by X-ray diffraction in $Ag_{2-y}V_4O_{11}$ cathodes that had been discharged to 3.0 V versus lithium. The formation of silver on the first voltage plateau ($x=0$–2) is also consistent with a decreasing R_{dc} in the early portion of discharge. Electron diffraction on the needle-shaped crystals of lithiated $Ag_{2-y}V_4O_{11}$ showed that diffraction lines occur rather than diffraction spots. An example of an electron diffraction pattern appears in Fig. 5. It was not possible to image these crystals along the long axis of the needles because of their preferred orientation and their thickness in the long direction. Ion milling, which was successful in producing samples of $Ag_{2-y}V_4O_{11}$ [5] which were thin in the needle direction, was unsuccessful in the case of the lithiated material, possibly because of the hygroscopic nature of the material and sensitivity to the electron beam.

Diffraction lines instead of spots indicate an almost complete loss of periodicity in one direction. The continuous diffraction lines make it difficult to determine the two remaining axes. The diffraction patterns also contain either incommensurate superreflections or the diffraction pattern of a second phase, as seen in Fig. 5. One set of diffraction lines can be roughly indexed with a unit plane of $a=15.3$ Å and $b=3.6$ Å. These two axes approximate the a and b dimensions of the unit cell of $Ag_{2-y}V_4O_{11}$ in both the Type I and Type II structural types, which differ in the stacking pattern of the V_4O_{11} layers. The retention of the basic layered structure and the appearance of silver on the surface of the particles suggest that silver is replaced by lithium during lithiation. The V_4O_{11} layers remain as rigid units in the a–b plane, with random stacking of the layers

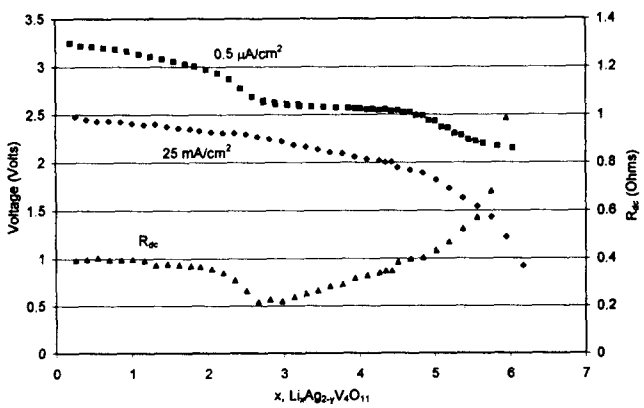

Fig. 3. Discharge behaviour of a $Li/Ag_{2-y}V_4O_{11}$ battery on a low current drain with high-current pulses imposed periodically. R_{dc} is calculated from the voltage drop during the pulse and the pulse current using Ohm's law.

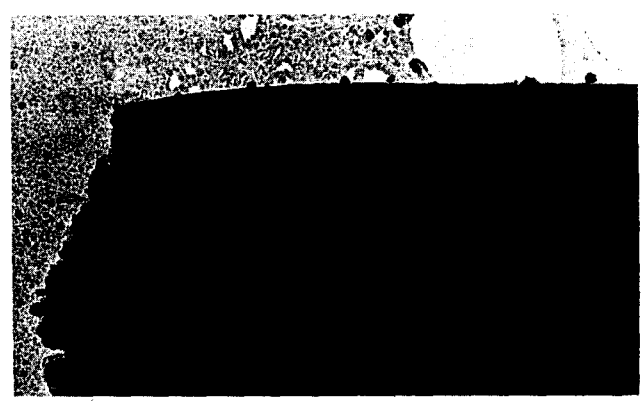

Fig. 4. Electron microscope image of $Li_3V_4O_{11}$, showing the presence of silver particles on the surface. Silver particles are also likely to occur in the interior of the crystal.

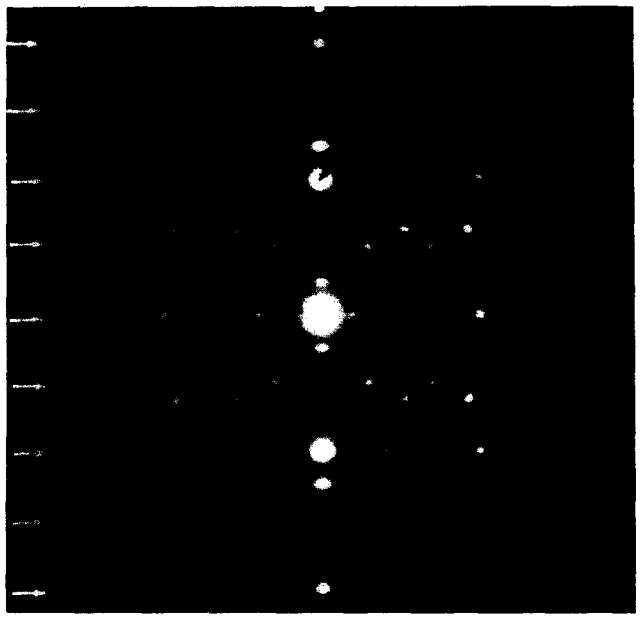

Fig. 5. Electron diffraction pattern of $Li_3V_4O_{11}$. The diffraction pattern is very complex. The diffraction spots on the rows indicated by the white arrows can be indexed with a centered unit cell with $a = 15.3$ Å and $b = 3.6$ Å. Half-way between these rows some extra weak spots occur indicating a doubling of the b-axis. On top of this pattern other spots occur which are incommensurate with the unit cell of $a = 15.3$ Å and $b = 3.6$ Å.

in the c direction. The interlayer spacing would be expected to decrease upon replacement of silver with lithium between the layers because of the smaller ionic radius of Li^+. However, because of the disordered stacking of the layers, this dimension could not be determined. The retention of the V_4O_{11} layers as the basic structural unit is also consistent with the reversibility of the lithiation reaction, as reported in Ref. [10].

4. Conclusions

The first step in the lithiation of $Ag_{2-y}V_4O_{11}$ is the reduction of silver accompanied by the replacement of silver with lithium in the oxide structure. The V_4O_{11} layers are retained, but the stacking of the layers becomes random. The production of metallic silver early in discharge is probably responsible for the decreasing battery resistance in the same region of cathode composition.

Acknowledgements

The authors thank Dr K. West of the Technical University of Denmark for discussions on the thermodynamics of $Li/Li_xAg_{2-y}V_4O_{11}$.

References

[1] E.S. Takeuchi and P. Piliero, *J. Power Sources, 21* (1987) 133–141.
[2] E.S. Takeuchi and W.C. Thiebolt III, *J. Electrochem. Soc., 135* (1988) 2691–2694.
[3] C.F. Holmes, P. Keister and E. Takeuchi, *Prog. Batteries Solar Cells, 6* (1987) 64–66.
[4] E.S. Takeuchi, M.A. Zelinsky and P. Keister, *Proc. 32nd Power Sources Symp.*, The Electrochemical Society, Pennington, NJ, USA, 1986, pp. 268–273.
[5] W. Zandbergen, A.M. Crespi, P.M. Skarstad and J.F. Vente, *J. Solid State Chem., 110* (1994) 167–175.
[6] A.M. Crespi, P.M. Skarstad, H.W. Zandbergen and J. Schoonman, *Proc. Symp. Lithium Batteries*, Proc. Vol. 93–24, The Electrochemical Society, Pennington, NJ, USA, 1993, pp. 98–105.
[7] R.A. Leising and E.S. Takeuchi, *Chem. Mater., 5* (1993) 738–742.
[8] J. Galy and D. Lavaud, *Acta Crystallogr., Sect. B, 27* (1971) 1005–1009.
[9] A.D. Wadsley, *Acta Crystallogr., 8* (1955) 695–701.
[10] K. West and A. Crespi, *J. Power Sources, 54* (1994) 334.
[11] E.S. Takeuchi and W.C. Thiebolt III, *J. Electrochem. Soc., 135* (1988) 2691–2694.